Pressure-dependence of electron-phonon coupling and the superconducting phase in hcp Fe - a linear response study

S. K. Bose,* O. V. Dolgov, J. Kortus, O. Jepsen, and O. K. Andersen

Max-Planck-Institute for Solid State Research, Heisenbergstr. 1, 70569 Stuttgart, Germany

A recent experiment by Shimizu *et al.* (Ref.1) has provided evidence of a superconducting phase in hcp Fe under pressure. To study the pressure-dependence of this superconducting phase we have calculated the phonon frequencies and the electron-phonon coupling in hcp Fe as a function of the lattice parameter, using the linear response (LR) scheme and the full potential linear muffin-tin orbital (FP-LMTO) method. Calculated phonon spectra and the Eliashberg functions $\alpha^2 F$ indicate that conventional s-wave electron-phonon coupling can definitely account for the appearance of the superconducting phase in hcp Fe. However, the observed change in the transition temperature with increasing pressure is far too rapid compared with the calculated results. For comparison with the linear response results, we have computed the electron-phonon coupling also by using the rigid muffin-tin (RMT) approximation. From both the LR and the RMT results it appears that electron-phonon interaction alone cannot explain the small range of volume over which superconductivity is observed. It is shown that ferromagnetic/antiferromagnetic spin fluctuations as well as scattering from magnetic impurities (spin-ordered clusters) can account for the observed values of the transition temperatures but cannot substantially improve the agreeemnt between the calculated and observed presure/volume range of the superconducting phase. A simplified treatment of p-wave pairing leads to extremely small ($\leq 10^{-2}$ K) transition temperatures. Thus our calculations seem to rule out both s- and p- wave superconductivity in hcp Fe.

I. INTRODUCTION

Recently Shimizu *et al.*[1] (see also Ref.2) have reported resistivity and magnetization measurements on Fe samples under pressure, and identified a superconducting phase characterized by the Meissner effect and the vanishing of the resistivity above a pressure of 15 GPa. At this pressure the stable crystal sructure of Fe is known to be hcp. Both the hcp phase and superconductivity in Fe under pressure are results that can be expected on theoretical grounds. Stability of bcc, fcc and hcp crystal structures as a function of canonical d-band filling was discussed some time back by Pettifor[3] and Andersen *et al.*.[4,5] These authors showed that without ferromagnetism the ground state of Fe would be hcp, just as for its nonmagnetic and isoelectronic 4d and 5d counterparts, Ru and Os. For Fe the bcc structure is stabilized only via ferromagnetism. In the ferromagnetic bcc state both the atomic volume and compressibility of Fe are anomalously large.[6] Application of a moderate pressure results in bcc to hcp martensitic transformation and loss of ferromagnetism.[4] Both Ru and Os are superconducting at low temperatures. Thus superconductivity in hcp Fe is hardly surprising.

What differentiates hcp Fe from Ru and Os is the presence of spin fluctuations. Both ferromagnetic and antiferromagnetic spin fluctuations are known to suppress superconductivity mediated via s-wave electron-phonon coupling. A notable example, where ferromagnetic spin fluctuations (paramagnons) are believed to suppress superconductivity completely, is fcc Pd. A large density of states (DOS) at the Fermi level, $N(0)$, in fcc Pd causes a large Stoner-enhanced paramagnetic susceptibility, leading to strong ferromagnetic spin fluctuations. Disorder-induced superconductivity in fcc Pd, due mainly to the reduction in $N(0)$ and therefore in spin fluctuations, has been claimed experimentally as well as discussed theoretically.[7,8,9] A similar effect could conceivably be achieved in fcc Pd under pressure, but is yet to be observed. The case for hcp Fe is somewhat different, since it is believed to be close to antiferromagnetic[10] or complex magnetic[11] instability. It was noted by Wohlfarth[12] that at the lowest pressures ($\sim$10 GPa) at which hcp Fe is stable, it should be close to an antiferromagnetic instability. He also suggested that the antiferromagnetic spin fluctuations might not be strong enough to suppress superconductivity in hcp Fe, particularly at elevated pressures, where reduction in $N(0)$ would cause spin fluctuations to eventually disappear. Antiferromagnetic spin fluctuations suppress s-wave superconductivity, while contributing to p/d-wave superconductivity. At present experimental evidence regarding the type of superconductivity (s-wave or otherwise) in hcp Fe is lacking.

One can estimate the T_c in hcp Fe by using simple scaling arguments and the observed superconducting transition temperature T_c of Ru (0.5 K) or Os (0.7 K) at normal pressure. Let us ignore spin fluctuations and consider the McMillan expression:

$$T_c = \frac{\Theta_D}{1.45} \exp\left\{ -\frac{1.04\,(1 + \lambda_{ph})}{\lambda_{ph} - \mu^*(1 + 0.62\lambda_{ph})} \right\}, \quad (1)$$

where Θ_D is the Debye temperature, μ^* is the Coulomb pseudopotential, and λ_{ph} is the electron-phonon coupling constant, given by $\lambda_{ph} = N(0)\langle I^2\rangle/M\langle\omega^2\rangle$. Considering $\mu^* = 0.1$, we get $\lambda_{ph} = 0.32$ for Ru ($\Theta_D = 600$ K, see Ref.6). To estimate λ_{ph} for hcp Fe, we assume

that the mean square electron-phonon(ion) matrix element $\langle I^2 \rangle$ and the effective spring constant $M \langle \omega^2 \rangle$ are nearly the same as in hcp Ru. The average phonon frequency, and thus Θ_D, should then scale as the inverse square root of the ratio of the atomic masses, and λ_{ph} should scale according to the ratio of $N(0)$. The quantity $N(0)$ can be easily calculated for elemental solids. However, we only need to estimate the ratio of this quantity between Ru and Fe. We can start by assuming that $N(0)$ is proportional to the inverse d-band width, which can be estimated from the potential parameters of the LMTO-ASA (atomic sphere approximation) method.[5] Here the band width is proportional to the potential parameter Δ. Both Δ and its volume derivative have already been tabulated[13] for a large number of elemental solids. From the d-orbital values of the parameter Δ, $N(0)_{Fe}/N(0)_{Ru} \simeq \Delta_{Ru}/\Delta_{Fe} = 539/280 = 1.925$. This would give λ_{ph} =0.62 for Fe, resulting in a transition temperature of $\sim$17 K for hcp Fe. If we use published values of $N(0)$, for hcp Fe[14] (corresponding to a pressure $P \sim$ 10 GPa) and for Ru[15] (corresponding to normal prssure), then $N(0)_{Fe}/N(0)_{Ru} = 20.8/11.8 = 1.76$, and λ_{ph} =0.56 for hcp Fe. This ratio yields an improved value $T_c(Fe)$ = 12 K. Using the measured value of Θ_D in hcp Fe ($\sim$ 500 K at $\sim$ 10 GPa, see Ref.16) gives a value[59] of 7.6 K.

For a quick estimate of the pressure-dependence of T_c we use a simplified version of Eq.1:

$$T_c = \frac{\Theta_D}{1.45} \exp\left(\frac{1}{\lambda'}\right) \ , \lambda' = \lambda_{ph} - \mu^* \ , \qquad (2)$$

and resort to the tabulated values of the logarithmic derivative of the potential parameter Δ with respect to atomic sphere radius, s (Ref.13). Neglecting the volume(pressure) dependence of the quantities $\langle I^2 \rangle$ and μ^* in Eq.2, we obtain, for the logarithmic derivative of T_c with respect to the system volume V:

$$\frac{d \ln T_c}{d \ln V} = -\gamma_G \left(1 - \frac{2}{\lambda_{ph}}\right) + \frac{1}{\lambda_{ph}} \frac{d \ln N(0)}{d \ln V} \ , \qquad (3)$$

where γ_G is the Grüneisen parameter. We have used the approximations:

$$\gamma_G = -\frac{d \ln \Theta_D}{d \ln V} \approx -1/2 \frac{d \ln \langle \omega^2 \rangle}{d \ln V} \ . \qquad (4)$$

With the assumption $N(0) \sim \Delta^{-1}$, where Δ is the d-orbital band width parameter in LMTO-ASA, $d \ln N(0)/d \ln V = -(1/3) d \ln \Delta/d \ln s$. For the d-orbitals of Fe $d \ln \Delta/d \ln s$ = -4.6. From the reported value[16] of $\gamma_G = 1.5$ in hcp Fe, we obtain a value $\frac{d \ln T_c}{d \ln V} = 6.6$ for hcp Fe. The zero pressure bulk modulus in hcp Fe is 165 GPa.[17] The initial (low pressure) logarithmic derivative of T_c in hcp Fe should thus be close to -6.6/165 (GPa)$^{-1}$ = - 4% /GPa.

Exercises such as the one outlined above are useful in obtaining order of magnitude estimates and in understanding the trend from one element to the next. However, quantitative agreement with experimental results might be missing. According to the study by Shimizu *et al.*[1] superconductivity in hcp Fe appears at around 15 GPa, slightly above the pressure at which the bcc-hcp transition takes place. The transition temperature grows slowly from below 1 K to about 2 K at $\sim$22 GPa and then decreases steadily, with superconductivity vanishing beyond 30 GPa.[18] The rate of decrease of T_c is too rapid compared with the estimate derived above. In order to reproduce the initial increase of T_c with pressure, as observed in the experiment, it would be necessary to include the spin fluctuation effects and possible volume dependence of the matrix element $\langle I^2 \rangle$. With inceasing pressure, spin fluctuations are expected to diminish, causing T_c to rise. The electron phonon matrix element may also increase with pressure, as the nearest neighbor distances become shorter. It would thus be of interest to examine to what extent the observed results can be explained via a rigorous *ab initio* calculation. To this end we have used the full-potential linear muffin-tin orbitals linear response (FP-LMTO-LR) scheme developed by Savrasov[19,20] to calculate the phonon frequencies and the electron-phonon coupling in hcp Fe as a function of pressure. The Eliashberg equations,[21] in their isotropic Fermi surface averaged form, are used to study the pressure-dependence of the transition temperature T_c, and the superconducting gap Δ. Effects of both ferromagnetic and antiferromagnetic spin fluctuations and the effects of scattering from magnetic impurities are explored to accommodate the experimental data as best as possible. We also present a simplified treatment of p-wave pairing in hcp Fe. So far two other theoretical calculations, related to superconductivity in hcp Fe and its pressure dependence, have appeared.[14,22] Our work differs from these publications[14,22] in asmuch as it presents a more rigorous first-principles calculation of the phonons and the electron-phonon coupling as a function of the lattice parameter in hcp Fe.

II. ELECTRONIC STRUCTURE

There is considerable experimental evidence that at room temperature the martensitic transition from the bcc to the hcp phase in iron takes place at a pressure of 10-15 GPa.[23,24,25] Recently Ekman *et al.*[26] have studied this phase transition using the full-potential linear augmented plane wave (FP-LAPW) total energy method. Their study indicates a first order ferromagnetic bcc to nonmagnetic hcp transition. These authors carried out spin-polarized density functional calculations using the generalized-gradient approximation (GGA) of Perdew and Wang (GGA1).[27] Steinle-Neumann *et al.*,[10] using a later version of the GGA by Perdew, Burke, and Ernzerhofer (GGA2),[28] find an antiferromagnetic ground state for hcp Fe and show that this version of the GGA better reproduces the observed elastic properties of hcp Fe under pressure. The possibility of noncollinear magnetism in hcp Fe below 50 GPa has also been suggested.[11] These

results are at variance with the Mössbauer study of hcp Fe under pressure, which has failed to reveal any local magnetic moment.[25,29] The possibility remains that hcp Fe stays close to antiferromagnetic or complex magnetic instability. In this work we assume a nonmagnetic phase for hcp Fe under pressure, and present results that were obtained by using GGA1.[27] Our calculations, using various forms of GGA, show that the nature of the ground state at various lattice parameters depends very much on the exchange correlation potential and the c/a ratio. In addition, the energy differences between nonmagnetic, ferromagnetic, and antiferromagnetic (AFM I and AFM II configurations[10]) states are often small (almost within the errors of the method), as well as dependent on technical details, such as the number of $\mathbf{k}$-points in the irreducible Brillouin zone and method of BZ integration (see further discussion in section V).

According to Ekman *et al.*[26] the bcc to hcp transition leads to a phase with a c/a ratio of 1.57. Our LMTO-ASA calculations yield a smaller (by ~ 0.8 mRy) hcp ground state energy for $c/a = 1.57$ than for the ideal close packing value. In the FP-LMTO calculations the difference in the ground state energies for the two c/a values is smaller than 0.2 mRy. Previous theoretical studies for iron indicate a very small dependence of the total energy on the c/a ratio[30,31] and in addition, the c/a ratio is likely to change with pressure. We have thus adopted the simplest option, as in Ref.14, and carried out all our calculations with the ideal close-packing case: $c/a = \sqrt{8/3}$. The electronic structure was calculated using Savrasov's FP-LMTO code[32] with a triple-κ *spd* LMTO basis for the valence bands. $3s-$ and $3p$-semicore states were treated as valence states in separate energy windows. The charge densities and potentials were represented by spherical harmonics with $l \leq 6$ inside the nonoverlapping MT spheres and by plane waves with energies ≤ 141 Ry in the interstitial region. Brillouin zone (BZ) integrations were performed with the full-cell tetrahedron method[33] using 793 $\mathbf{k}$-points in the irreducible zone. Band structures of hcp Fe obtained via the FP-LMTO method for all lattice parameters considered are in good agreement with the LMTO-ASA bands. FP-LMTO bands for the ideal c/a ratio and lattice parameter of 4.6 a.u. are shown in Fig. 1.

Table I shows the lattice parameters used in our calculations together with the atomic volumes and some calculated properties. Pressure ($-\partial E/\partial V$) and bulk modulus were calculated by fitting the energy vs. lattice parameter curve to the generalized Birch-Murnaghan equation of state.[34,35] The equilibrium atomic volume and bulk modulus, 69.4 a.u. and 290 GPa, compare well with the values obtained by the FP-LAPW calculations of Ekman *et al.*[26] (68.94 a.u. and 263 GPa). Calculated pressure and bulk modulus values become progressively less reliable away from the equilibrium volume. In order to calculate the Stoner parameter I we introduced a small splitting in the self-consistent paramagnetic bands by adding small up and downward shifts to the band-
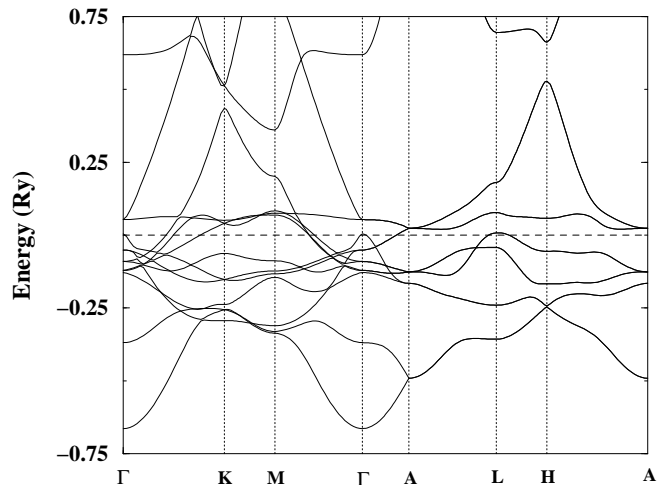

FIG. 1: FP-LMTO energy bands in hcp Fe for the ideal c/a value ($\sqrt{8/3}$), and a= 4.6 a.u. The horizontal line shows the position of the Fermi level, chosen as the zero of energy.

TABLE I: FP-LMTO results for nonmagnetic hcp Fe for the ideal c/a ratio: a= lattice parameter (a.u.), V_0 = volume per atom (a.u.), P=pressure (GPa), B=Bulk Modulus (GPa), $N(0)$= DOS at the Fermi level (states/(Ry atom spin)), I= Stoner parameter (Ry/atom).

a	4.0	4.2	4.4	4.5	4.6	4.7
V_0	45.25	52.39	60.23	64.44	68.83	73.41
P	350	162	56	26	2.3	-14
B	1695	970	550	410	300	221
$N(0)$	4.77	5.79	7.05	7.80	8.59	9.46
I	0.074	0.074	0.073	0.073	0.073	0.075
$1/(1-IN)$	1.54	1.75	2.06	2.32	2.68	3.44

center parameter C in the LMTO-ASA method. After making the atom self-consistent the Stoner parameter I was calculated from the induced magnetic moment per atom μ, assuming proportionality between band-splitting and the Stoner parameter:

$$I = \sum_l I_l \delta_l; \ I_l = (C_l^\uparrow - C_l^\downarrow)/\mu; \ \delta_l = N_l(0)/N(0) \, , \quad (5)$$

where the arrows indicate spin-up and down states and $N_l(0)$ and $N(0)$ are the l-partial and total DOSs at the Fermi level, respectively. This method yields almost the same (pressure-independent) value as that obtained by Mazin *et al.*.[14] Both our method and that used in Ref.14 can be called fixed spin-moment method, except that Mazin *et al.* derived I from the second derivative of the total energy with respect to the spin-moment.

III. LATTICE VIBRATIONS AND ELECTRON-PHONON COUPLING

We used the linear response code of Savrasov[19,20] with a triple-κ LMTO basis set. The dynamical matrix was generated for 28 phonon wave vectors in the irreducible BZ, corresponding to a mesh of (6,6,6) reciprocal lattice divisions. The BZ integration for the dynamical matrix was done for a mesh of (12,12,12) reciprocal lattice divisions, and that for the electron-phonon (Hopfield) matrix was done for a (24,24,24) mesh. The calculated phonon spectra for two lattice parameters, 4.4 a.u. and 4.0 a.u., are shown in Fig.2. Our results are in reasonable agreement with a recent density functional calculation of Alfé *et al.*[36] These authors use the same GGA as is used in our calculation (GGA1)[27] and the small displacement method[37] to obtain the force constant matrix. In Fig.3 of their paper the phonon spectra for two volumes 8.67 Å^3 and 6.97 Å^3 are shown. The corresponding lattice parameters, 4.36 a.u. and 4.05 a.u., are close to the values for which our calculated phonon dispersions curves are shown in Fig. 2. The phonon frequencies at the Γ and A points agree remarkably well. Some differences appear at symmetry points K and M. Such differences are also present between the results of Alfé *et al.*[36] and those obtained by Söderland *et al.* using a generalized pseudopotential parameterization[30] of FP-LMTO calculations. The differences between our LR results and those of Alfé *et al.*[36] are not large enough to cause significant differences in thermal properties and electron-phonon coupling. The smooth solid lines in Fig. 2 correspond to spline fits to the calculated frequencies (solid circles). Due to the small number of calculated frequencies the shapes of the lines presumably representing the bands at the zone boundaries could be incorrect. The connections of the calculated points with lines and band crossings in Fig. 2 were determined by examining the phonon eigenvectors. However, the number of **q**-points considered along each symmetry direction was at most four and often three or less. No intermediate **q**-points along the K - M and L - H were among the mesh of **q**-points for which the dynamical matrix was calculated. Thus the possibility of errors in band crossing cannot be ruled out.

The dispersion curves at various pressures are similar, except for an overall scale factor, essentially representing the gradual broadening of the bands with increasing pressure. This is reflected in Fig. 2 and also in the phonon density of states for various lattice parameters shown in part (b) of Fig. 4. For the smallest lattice parameter considered by us the upper band edge lies around 670 cm^{-1} or 20 THz (Fig. 2 and Fig. 4 (b)).

We have computed both the Eliashberg spectral function

$$\alpha^2 F(\omega) = \frac{1}{N(0)} \sum_{\mathbf{k},\mathbf{k}',ij,\nu} |g_{\mathbf{k},\mathbf{k}'}^{ij,\nu}|^2 \delta(\varepsilon_{\mathbf{k}}^i) \delta(\varepsilon_{\mathbf{k}'}^j) \delta(\omega - \omega_{\mathbf{k}-\mathbf{k}'}^\nu),$$
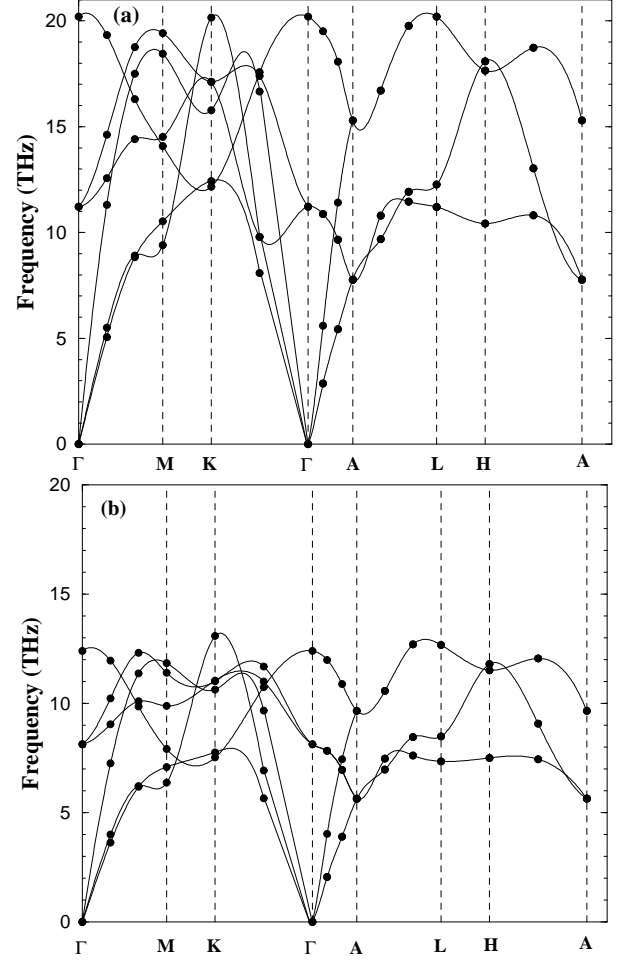(6)

FIG. 2: Phonon frequencies of hcp Fe calculated via FP-LMTO-LR method for two different lattice parameters: (a) 4.0 and (b) 4.4 a.u., and the ideal c/a ratio, $\sqrt{8/3}$. The solid circles denote the calculated frequencies and the solid lines represent spline fits through these calculated values.

and the transport Eliashberg function[20,38]

$$\alpha_{tr}^2 F = \frac{1}{2N(0)\langle v_F^2 \rangle} \sum_{\mathbf{k},\mathbf{k}',ij,\nu} |g_{\mathbf{k},\mathbf{k}'}^{ij,\nu}|^2 \left(\vec{v}_F(\mathbf{k}) - \vec{v}_F(\mathbf{k}') \right)^2$$
$$\times \delta(\varepsilon_{\mathbf{k}}^i) \delta(\varepsilon_{\mathbf{k}'}^j) \delta(\omega - \omega_{\mathbf{k}-\mathbf{k}'}^\nu),$$
(7)

where the subscript F denotes the Fermi surface, the angular brackets denote the Fermi surface average, $\vec{v}_F$ denotes the Fermi surface velocity, $g_{\mathbf{k},\mathbf{k}'}^{ij,\nu}$ is the electron-phonon matrix element, with ν being the phonon polarization index and $\mathbf{k}, \mathbf{k}'$ representing electron wave vectors with band indices i, and j, respectively.

For most of the lattice parameters considered by us the Eliashberg spectral function $\alpha^2 F$ and the transport Eliashberg function $\alpha_{tr}^2 F$ both follow the same frequency variation as the phonon density of states. In Fig.3 we show the phonon density of states and the two Eliashberg functions together with the phonon dispersions for the lattice parameter 4.6 a.u., close to the equilibrium value

of 4.615 a.u.

Some deviations in the frequency dependence of the $\alpha^2 F$ function from that of the phonon density of states appear at higher pressure. The deviation is most pronounced between the lattice parameters 4.4 and 4.2 a.u. in our calculation. In Fig.4 we show the Eliashberg spectral functions and the phonon density of states for three different lattice parameters. The peaks in the calculated phonon density of states at ambient pressure (lattice parameter $\sim$ 4.6 a.u. in our calculations) are at 190 cm^{-1} (24 meV) and 315 cm^{-1} (39 meV), and these agree very well with the results from neutron scattering experiments[39] as well as with recently reported results, obtained from the measured energy spectra of inelastic nuclear absorption.[16] The peak positions in the calculated results for higher pressures are at somewhat lower frequencies (by about 5 meV, which is within the experimental resolution) than those from the inelastic nuclear absorption experiment.[16] However, such differences between the calculated and measured frequencies are common, given the difference between the experimental and theoretical values of the lattice parameters at various pressures.

The Hopfield parameter η $(N(0)\langle I^2 \rangle)$, which is the electronic part of the electron-phonon coupling, shows an above average increase between the lattice parameters 4.5 and 4.4 a.u., due to an increased coupling for the longitudinal acoustic phonons with wave vectors around the middle of the Γ- K symmetry line. This increased (above average) coupling is found to persist up to at least 4.2 a.u., but diminishes to normal (average) value around the lattice parameter of 4.0 a.u., where the pressure-stiffening of the lattice vibrations reduces the electron-phonon coupling and superconductivity disappears. The general trend is as follows: the Hopfield parameter η grows steadily with increasing pressure with a rapid change between the lattice parameters 4.5 and 4.4 a.u. The phonon frequencies move upward with increasing pressure, with no phonon branches showing any softening. However, between lattice parameters 4.6 a.u. and 4.4 a.u. (perhaps 4.3 a.u.) the increase in the Hopfield parameter dominates the change in the electron-phonon coupling parameter $\lambda_{ph} = \eta / M \langle \omega^2 \rangle$. In this range λ_{ph} increases despite a decrease in $N(0)$ and an increase in $\langle \omega^2 \rangle$. Below 4.3 a.u. lattice vibrations stiffen rapidly, lowering the value of λ_{ph}. In Table II we summarize our results for the pressure-dependence of the phonon properties and electron-phonon coupling. Since the Hopfield parameter η is often calculated using the rigid muffin-tin (RMT) approximation of Gaspari and Gyorffy,[40] in Table II we have also presented the results for η obtained via the LMTO-ASA implementation of RMT (rigid atomic sphere or RSA) as given by Glötzel et al.[41] and Skriver and Mertig.[42] These values are in agreement with those given by Mazin et al.,[14] but differ significantly from the results of Jarlborg[22] (judging from the quoted values of λ_{ph} and the Debye frequencies). Our results indicate that depending on the lattice parameter the RMT/RSA ap-

proximation underestimates the Hopfield parameter by 15-45%. Also the variation of η with lattice parameter in the RMT approximation is much smoother than in the linear response calculation, as the former fails to capture the above average increase around the lattice parameter 4.4 a.u. In Table II we have presented the results for lattice parameter 4.7 a.u. merely for comparison with other lattice parameters, and not for comparison with experiment. The strong electron-phonon coupling (stronger than that at a =4.6 a.u.) is of no experimental consequence since, (i) at this lattice parameter the system is at a negative pressure, not accessed by experiment; and (ii) our theoretical calculations show that at this expanded volume the system is most likely antiferromagnetic.

IV. CRITICAL TEMPERATURE

A. General relations

The linearized Eliashberg equations at the superconducting transition temperature T_c of an isotropic system are (see, e.g., Ref.21):

$$Z(i\omega_n) = 1 + \frac{\pi T_c}{\omega_n} \sum_{n'} W_+(n-n')\mathrm{sign}(n'), \quad (8)$$

$$Z(i\omega_n)\Delta(i\omega_n) = \pi T_c \sum_{n'}^{|\omega_n| \ll \omega_c} W_-(n-n')\frac{\Delta(i\omega_{n'})}{|\omega_{n'}|},$$

where $\omega_n = \pi T_c(2n+1)$ is a Matsubara frequency, $\Delta(i\omega_n)$ is an order parameter and $Z(i\omega_n)$ is a renormalization factor. Interactions

$$W_+(n-n') = \lambda_{ph}(n-n') + \lambda_{sf}(n-n') + \delta_{nn'}(\gamma_n + \gamma_m),$$

and

$$W_-(n-n') = \lambda_{ph}(n-n') - \lambda_{sf}(n-n') - \mu^*(\omega_c) + \delta_{nn'}(\gamma_n - \gamma_m),$$

contain a phonon contribution

$$\lambda_{ph}(n-n') = \int_0^\infty \frac{d\omega^2 \alpha^2(\omega)F(\omega)}{(\omega_n - \omega_{n'})^2 + \omega^2} \, ,$$

where $\alpha^2(\omega)F(\omega)$ is the so-called Eliashberg spectral function, and a contribution connected with spin fluctuations

$$\lambda_{sf}(n-n') = \int_0^\infty \frac{d\omega^2 P(\omega)}{(\omega_n - \omega_{n'})^2 + \omega^2} \, .$$

$P(\omega)$ is the spectral function of spin fluctuations, related to the imaginary part of the transversal spin susceptibility $\chi_\pm(\omega)$ as

$$P(\omega) = -\frac{1}{\pi} \left\langle |g_{\mathbf{k}\mathbf{k}'}|^2 \mathrm{Im}\chi_\pm(\mathbf{k}, \mathbf{k}', \omega) \right\rangle \, ,$$
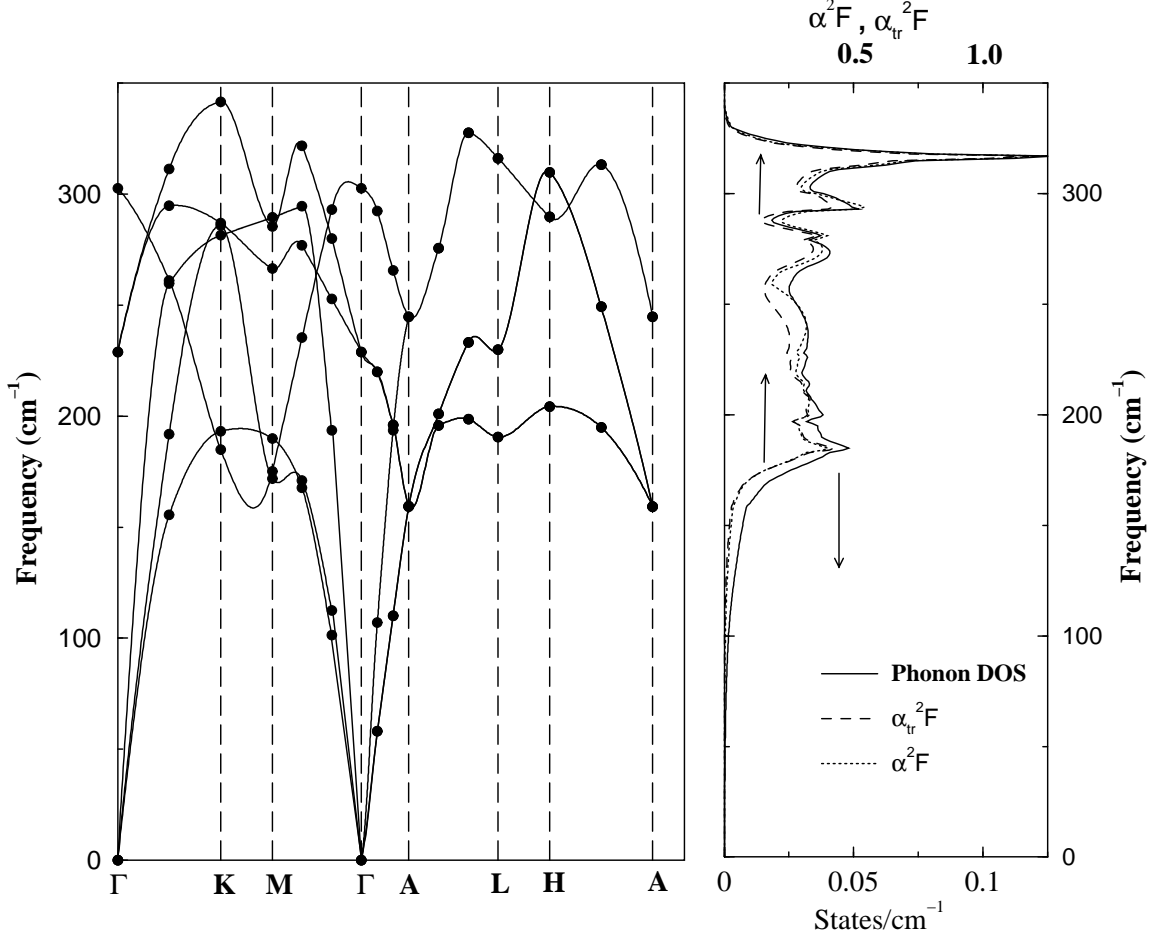
FIG. 3: Phonon spectrum, density of states and the Eliashberg spectral function $\alpha^2 F$ and the transport Eliashberg function $\alpha^{2,xx}_{tr} F$ for hcp Fe at the lattice parameter 4.6 a.u. (c/a=$\sqrt{8/3}$). The equilibrium (minimum energy) lattice parameter is 4.615 a.u.

and $\mu^*(\omega_c)$ is the screened Coulomb interaction

$$\mu^*(\omega_c) = \frac{\mu}{1 + \mu \ln(E/\omega_c)}, \qquad (9)$$

where $\mu = \langle N(0)V_c \rangle_{FS}$ is the Fermi surface averaged Coulomb interaction. E is a characteristic electron energy, ω_c is a cut-off frequency, usually chosen ten times the maximum phonon frequency: $\omega_c \simeq 10\omega_{ph}^{\max}$. $\gamma_n = 1/2\tau_n, \gamma_m = 1/2\tau_m$ are scattering rates for nonmagnetic and magnetic impurities, respectively.

B. Phonons only

In order to compute T_c we use the calculated Eliashberg spectral function along with the following procedure to determine the Coulomb pseudopotential $\mu^*(\omega_c)$. We start by assuming $\mu = 0.5$. A value greater than 0.5 for μ would lead to magnetic instability (see, e.g. Ref.43). With $E = \omega_{pl}$, the electron plasma frequency

(see Ref.44),

$$\mu^*(\omega_c) = \frac{0.5}{1 + 0.5 \ln(\omega_{pl}/\omega_c)} \ .$$

Thus from the calculated phonon frequencies and plasma frequencies we obtain μ^* for all lattice parameters, with the cut-off frequency ω_c assumed to be ten times the maximum phonon frequency. This procedure gives us the maximum possible values of $\mu^*(\omega_c)$.

One of the most widely used expressions for T_c is given by the Allen-Dynes form[21] of the McMillan formula (Eq.1), where the prefactor $\Theta_D/1.45$ is replaced by $\omega_{\ln}^{ph}/1.2$.

$$\lambda_{ph} = 2 \int_0^\infty d\omega \alpha^2(\omega) F(\omega)/\omega$$

is the electron-phonon coupling constant, $\omega_{\ln}^{ph}$ is a logarithmically averaged characteristic phonon frequency

$$\omega_{\ln}^{ph} = \exp\left\{ \frac{2}{\lambda_{ph}} \int_0^\infty d\omega \alpha^2(\omega) F(\omega) \ln \omega/\omega \right\},$$

TABLE II: Hopfield parameters from the linear response calculation η and the rigid muffin-tin (atomic sphere) approximation η (RMT/RAS), mean square electron-ion matrix element $\langle I^2 \rangle$, calculated average plasma frequencies ω_{pl}, logarithmic average phonon frequencies ω_{ln}, cutoff frequencies ω_c, Coulomb pseudopentials for Eliashberg equation ($\mu^*(\omega_c)$) and McMillan formula (μ_{ln}^*); electron-phonon coupling parameters λ_{ep}, calculated critical temperatures (T_c^{calc}) and superconducting gaps (Δ_0) from the solution of the Eliashberg equations (8) and the critical temperatures from the McMillan formula (1)(T_c^{McM}) for various lattice parameters a.

| a	a_B	4.0	4.2	4.4	4.5	4.6	4.7
η	Ry/bohr^2	0.268	0.368	0.229	0.139	0.111	0.099
η (RMT/RAS)	Ry/bohr^2	0.214	0.167	0.124	0.108	0.095	0.088
$\langle I^2 \rangle$	(Ry/bohr)^2	0.056	0.063	0.032	0.018	0.013	0.010
ω_{pl}	eV	10.30	8.82	7.68	7.21	6.78	6.40
ω_{ln}	K	640	542	439	372	336	295
	cm^{-1}	445	376	305	258	233	205
ω_c	cm^{-1}	7000	6000	4600	4600	4600	4490
$\mu^*(\omega_c)$		0.224	0.224	0.218	0.221	0.224	0.226
$\mu^*(\omega_{ln})$		0.139	0.138	0.137	0.135	0.134	0.133
λ_{ph}		0.277	0.570	0.538	0.434	0.431	0.508
T_c^{McM}	K	< 0.01	6.37	4.06	1.06	0.94	2.21
T_c^{calc}	K	$5 \cdot 10^{-7}$	4.52	3.11	0.83	0.66	1.73
Δ_0	cm^{-1}	< 10^{-6}	7.38	4.63	1.28	0.99	2.54
$\Delta_0/k_B T_c^{calc}$			2.35	2.15	2.21	2.14	2.30
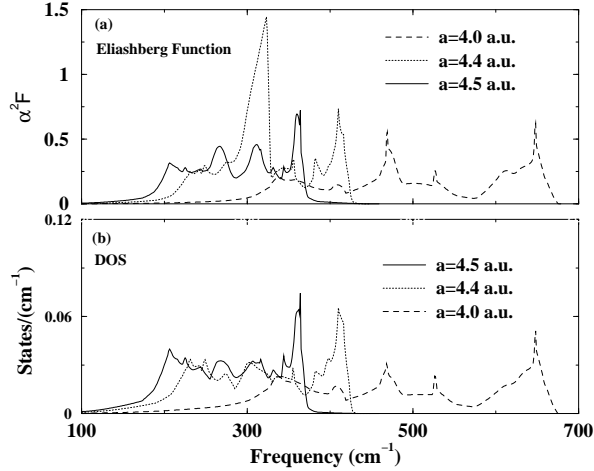
FIG. 4: Phonon density of states and the Eliashberg function for hcp Fe for three different lattice parameters (c/a=$\sqrt{8/3}$).

and

$$\mu^* \equiv \mu^*(\omega_{ln}^{ph}) = \frac{\mu^*(\omega_c)}{1 + \mu^*(\omega_c) \ln(\omega_c/\omega_{ln}^{ph})}$$

is the Coulomb pseudopotential at this frequency. Our calculations show that for different plasma frequencies and characteristic phonon frequencies μ^* for all lattice parameters lies in the range $0.13 - 0.14$, which is typical of conventional superconductors.

In Fig.5 we show the transition temperatures calculated as a function of volume per atom using Eliashberg equations and the McMillan formula. The effects of ferromagnetic and antiferromagnetic spin fluctuations, discussed in the following subsection, are also shown via three additional curves. The symbols denote the calculated values of T_c and the lines are spline fits through the calculated values.

C. Contribution from spin fluctuations

Superconducting transition temperatures calculated in the previous subsection are based on the maximum possible estimates of the Coulomb pseudopotential μ^*. Thus T_c, based on s-wave electron-phonon interaction only, cannot be less than 4.5 K, and a value as high as 7-8 K is reasonable according to the linear response results. The highest transition temperature obtained in the experiment[1] is 2 K. A more important difference between the calculated and the experimental results is the range of volume/pressure over which superconductivity appears. The calculated range is much broader than the experimental one (see Fig.5). It is then natural to explore the effects of spin fluctuations on both, the magnitude of T_c and the pressure/volume range of the superconducting phase. Since the calculation of the spin succeptibility is rather complicated, we restrict ourselves to simple models of *ferromagnetic* and *antiferromagnetic* spin fluctuations for an isotropic system, as proposed by Mazin *et al.*.[14] In a $T-$ matrix approximation for the uniform
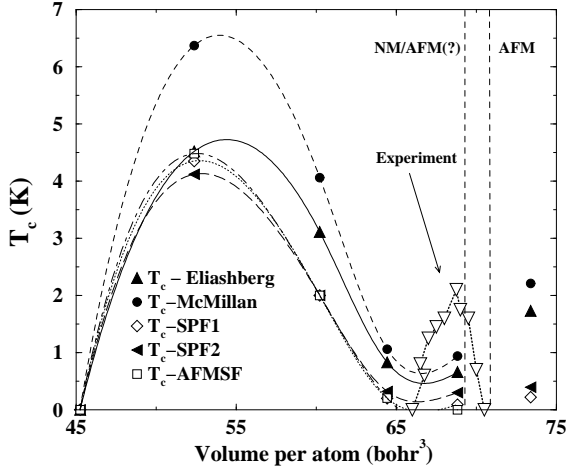
FIG. 5: Calculated transition temperatures for various volumes per atom. The experimental results are also shown. The experimental pressure versus T_c results were transferred into volume versus T_c results using the data from Mazin *et al.*[14] (see also Refs.45,46). The legends SPF1, SPF2, and AFMSF are described in section IV. C. Dashed vertical lines show regions, where hcp Fe is known to be antiferromagnetic (AFM), and where it is either nonmagnetic (NM) or antiferromagnetic (AFM).

electron gas one can obtain the relation (see Refs.47,48):

$$P(\omega) = N(0) \int_0^{2p_F} dq \frac{q}{2p_F^2} \left\{ -\frac{1}{\pi} \text{Im} \chi_{\pm}(q, \omega) \right\},$$

where

$$-\frac{1}{\pi} \text{Im} \chi_{\pm}(q, \omega) = \frac{I}{\pi} \left[\frac{\pi}{2} I N(0) \frac{\omega}{qv_F} \right] / \left[\left(1 - IN(0) - IN(0) \frac{q^2}{12p_F^2} \right)^2 + \left(\frac{\pi}{2} IN(0) \frac{\omega}{qv_F} \right)^2 \right].$$

An integration of $P(\omega)$ (see section A.) leads to the spin fluctuation coupling parameter

$$\lambda_{sf} = \alpha N(0) I \ln \frac{1}{1 - N(0)I}, \qquad (10)$$

where the constant α is of order unity. One can define

$$\omega_{\ln}^{sf} = \exp \frac{2}{\lambda_{sf}} \int_0^\infty d\omega P(\omega) \ln \omega / \omega$$
$$\approx (0.8) \frac{[1 - IN(0)]}{IN(0)} p_F v_F \qquad (11)$$

as a characteristic spin fluctuation frequency, which should vanish near the magnetic phase transition. p_F, and v_F are the Fermi momentum and velocity, respectively. The product $p_F v_F$ can be replaced by $2E_F$ and estimated from the location of the Fermi energy with respect to the bottom of the band.

If we resort to the approximation

$$P(\omega) = (\lambda_{sf} \omega_{sf}/2)\delta(\omega - \omega_{sf}),$$

then for $\omega_{sf} \gg \omega_{ph}$ we obtain an extension of the McMillan formula, similar to the one used in Ref.14

$$T_c = \frac{\omega_{\ln}^{ph}}{1.2} \exp \left\{ -\frac{1.04(1 + \lambda_{ph} + \lambda_{sf})}{\lambda_{ph} - \lambda_{sf} - \mu^*[1 + 0.62(\lambda_{ph} + \lambda_{sf})]} \right\}. \qquad (12)$$

In reality the spectrum $P(\omega)$ is distributed from zero up to electronic energies. Near the phase transition the characteristic frequency is comparable to the characteristic phonon frequencies. An appropriate treatment of the broadness of the spectrum $P(\omega)$ leads to the replacement of the $\omega_{\ln}^{ph}$ in the above expression by

$$\omega = \omega_{\ln}^{sf} (\omega_{\ln}^{ph}/\omega_{\ln}^{sf})^\nu, \qquad (13)$$

with the exponent ν (see Ref.48) given by

$$\nu = \frac{\lambda_{ph}^2}{(\lambda_{ph} - \lambda_{sf}) \left[\lambda_{ph} - \lambda_{sf} + \frac{\lambda_{ph}\lambda_{sf}}{1+\lambda_{ph}+\lambda_{sf}} \ln[\omega_{\ln}^{ph}/\omega_{sf}] \right]}.$$

In the uniform electron gas approximation the constant α in Eq. (10) is of the order of unity. But such a high value of α in our calculation would cause the critical temperatures to vanish for all lattice parameters ($\lambda_{ph} < \lambda_{sf}$). It is evident that the uniform electron gas approximation would be inappropriate for a transition metal like iron. Hence we use the following approach: we consider α as a fitting parameter to get a $T_c = 2$ K, the experimental value, for the lattice parameter 4.4 a.u. (volume per atom ~ 60 a.u. The two sets of T_c versus lattice parameter results obtained this way are shown in Fig.(5) and are labeled as SPF1 and SPF2, respectively (the lowermost curves). In particular, SPF1 refers to the case where Eq. (12) is used with λ_{sf} given by Eq. (10); and SPF2 refers to the case where ω from Eq. (13) replaces $\omega_{\ln}^{ph}$ in Eq.(12), with λ_{sf} still given by Eq. (10). In Table III, the spin fluctuation coupling parameters associated with the results SPF1 and SPF2 in Fig. 5 are labeled as λ_{sf1} and λ_{sf2}, respectively. The values of the parameter α (see Eq.(10)) for the two cases SPF1 and SPF2 are 0.101 and 0.029, respectively. Calculated transition temperatures for the two models SPF1 and SPF2 are denoted by T_{c1}^{sf} and T_{c2}^{sf} in Table III, which also shows the characteristic spin fluctuation frequencies $\omega_{\ln}^{sf}$ for various lattice parameters.

For *antiferromagnetic* spin fluctuations the spin susceptibility has a maximum at $\mathbf{q} \to \mathbf{Q}^*$, and the averaging over the Fermi surface leads to

$$\lambda_{sf} \approx \frac{\chi(\mathbf{q} \to \mathbf{Q}^*)I}{1 - \chi(\mathbf{q} \to \mathbf{Q}^*)I}.$$

If, according to Mazin *et al.*,[14] we suppose $\chi(\mathbf{q} \to \mathbf{Q}^*) = bN(0)$, then

TABLE III: Spin fluctuation effects: ferromagnetic spin fluctuation coupling parameters $\lambda_{sf1}, \lambda_{sf2}$ (see text in section IV. C. for details); antiferromagnetic spin fluctuation coupling parameter λ_{sf}^{af}, the characteristic spin fluctuation frequency ω_{ln}^{sf}, and the corresponding critical temperatures T_{c1}^{sf}, T_{c2}^{sf}, and $T_{c,sf}^{af}$ (see text in section IV. C. for details).

a	a_B	4.0	4.2	4.4	4.5	4.6	4.7
ω_{ln}^{sf}	eV	33.48	22.56	14.80	11.39	8.59	5.67
λ_{sf1}		0.0155	0.024	0.038	0.048	0.062	0.0886
λ_{sf2}		0.0044	0.0069	0.011	0.0139	0.018	0.025
λ_{sf}^{af}		0.0036	0.0057	0.011	0.019	0.05	
T_{c1}^{sf}	K	0.0005	4.35	2	0.202	0.091	0.224
T_{c2}^{sf}	K	0.0019	4.12	2	0.324	0.303	0.398
T_c^{af}	K	0.0023	4.48	2	0.206	0.004	0

$$\lambda_{sf}^{af} = \frac{\alpha' b N(0) I}{1 - b N(0) I}, \qquad (14)$$

Parameter b can be estimated from the condition of the antiferromagnetic instability $bN(0)I \to 1$. This leads to $b \lesssim 1.5$ which is close to the value in Ref.14. Taking this value and using α' as a fitting parameter we obtain the result plotted in Fig. 5. $\alpha' = 0.0032$ reduces the maximum T_c (at 4.4 a.u.) to the experimental value, 2 K (for simplicity we used Eq.(12), with ω_{ln}^{ph} replaced by ω given by Eqns. (11) and (13), and λ_{sf}^{af} replacing λ_{sf}). The corresponding results are plotted in Fig.(5) and are labeled as AFMSF. The values of T_c and spin fluctuation coupling parameters are also shown in Table III, labeled as T_c^{af} and λ_{sf}^{af}, respectively. It is evident that the volume dependence of T_c obtained this way is very similar for ferromagnetic and antiferromagnetic spin fluctuations.
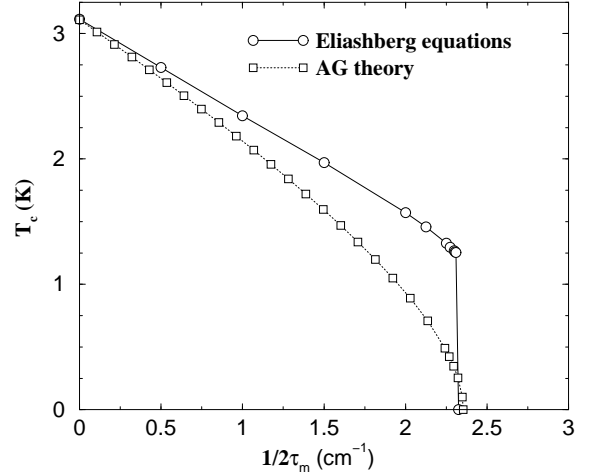

FIG. 6: Variation of the transition temperature with the scattering rate of magnetic impurities $1/2\tau_m$ for lattice parameter a =4.4 a.u. The legend AG stands for solution of the Abrikosov-Gor'kov expression given by Eq.(15).

D. Magnetic impurities

A lowering of the critical temperature could also be caused by the presence of magnetic impurities. It is well-known that the nonmagnetic impurities cancel out from the Eliashberg equations (Anderson theorem[49]), while the magnetic ones lead the pair-breaking effects.[50] The central idea is that near a magnetic transition spin- ordered clusters appear, and these can scatter electrons very effectively. We have calculated the effect of such impurities on the critical temperature for the lattice parameter $a = 4.4$ a.u. (see, Fig. 6) by considering various different scattering rates $1/2\tau_m$ in the Eliashberg Eq.(8). For comparison we have also calculated the change in T_c by using the renormalized Abrikosov-Gor'kov (AG) expression (see e.g., section 15 in Ref.21)

$$\ln(T_{c0}/T_c) \simeq \psi\left[1/2 + (1/2\tau_m)\pi T_c(1 + \lambda_{ep})\right] - \psi(1/2), \qquad (15)$$

where T_{c0} is the critical temperature without magnetic impurities. $\psi(x)$ is the digamma function and $\psi(1/2)$ is related to the Euler constant γ as $\psi(1/2) = -\gamma - 2\ln 2$. The difference between the Eliashberg and the AG results is due to the rather broad phonon spectrum which necessitates appropriate treatment of strong coupling effects.

In order to reduce the critical temperature at the lattice parameter $a = 4.4$ a.u. to the experimental value of 2 K it is sufficient to assume a scattering rate $1/\tau_m \approx 3.0$ cm^{-1}. With the calculated average Fermi velocity $v_F \simeq 2.547 \times 10^7$ cm/sec, this yields a mean free path $l \simeq 28.3 \times 10^{-5}$ cm. The closer the magnetic instability, the larger is the probability (rate) of magnetic scattering, which leads to more enhanced suppression of T_c.

E.   p-wave pairing

Magnetic ordering (as well as an external magnetic field) favors the triplet p-wave pairing, similar to that found in superfluid ^{3}He. In order to estimate T_c for p-wave pairing we adopt the following simplified approach. We consider the extension of Eq. (8) for the lth spherical harmonic channel[21]:

$$Z(i\omega_n) = 1 + \frac{\pi T_c}{\omega_n} \sum_{n'} W_+^{(0)}(n - n')\text{sign}(n'), \quad (16)$$

$$\mathbf{d}^{(l)}(i\omega_n) = \pi T_c \sum_{n'}^{|\omega_n| \ll \omega_c} W_-^{(l)}(n - n')\frac{\mathbf{d}^{(l)}(i\omega_{n'})}{Z(i\omega_{n'})|\omega_{n'}|},$$

where $\mathbf{d}^{(l)}$ for $l = 1$ is the p-wave order parameter, and

$$W_+^{(l)}(n - n') = \lambda_{ph}^l(n - n') + \lambda_{sf}^l(n - n') + \delta_{l0}\delta_{nn'}(\gamma_n + \gamma_m);$$

$$W_-^{(l)}(n - n') = \lambda_{ph}^l(n - n') + (-1)^l\lambda_{sf}^l(n - n') + \delta_{l0}X,$$

where $X = -\mu^*(\omega_c) + \delta_{nn'}(\gamma_n - \gamma_m)$. The kernel W with a general index l is defined as the Fermi surface (FS) average

$$W^{(l)} = \left\langle \mathbf{d}^{(l)} W(\mathbf{k}, \mathbf{k}', n - n)\mathbf{d}^{(l)} \right\rangle_{\mathbf{k},\mathbf{k}'\in FS} / \left\langle \left|\mathbf{d}^{(l)}\right|^2 \right\rangle$$

of the lth harmonic of the momentum-dependent interaction $W(\mathbf{k}, \mathbf{k}', n - n)$, while

$$W^{(0)} = \left\langle W(\mathbf{k}, \mathbf{k}', n - n) \right\rangle_{\mathbf{k},\mathbf{k}'\in FS}.$$

We assume that the Coulomb interaction and impurity scattering are isotropic. The simplest approximation then is to use $W^{(1)} = gW^{(0)}$, where the parameter g describes the anisotropy of the interaction (see, e.g., Refs.51,52). A difference of the factor g from unity leads to strong pair-breaking effects. In general (see., e.g. Ref.21), for $l = 1$ $\mathbf{d}^{(l)} \approx \mathbf{v}_F$, the first odd Fermi surface harmonic.[53] In this case $g = \lambda_{ph}^1/\lambda_{ph}^0 = \lambda_{ph}^{(in)}/\lambda_{ph}$ (see notations in Refs.38,20). The phonon constant $\lambda_{ph}^{(in)}$ is relevant to the transport Boltzmann equation (see, e.g., Ref.20). From the linear response calculation we obtain $g = \lambda_{ph}^{(in)}/\lambda_{ph}$ for all lattice parameters. For a=4.4 a.u., we obtain g=0.238.

With the assumption $W^{(1)} = gW^{(0)}$ it is possible to estimate T_c from a McMillan-like formula. An expression for the critical temperature can be written in a form similar to that used by Mazin et al.[14]:

$$\begin{aligned}
T_c &= \frac{\omega}{1.2} \exp\left\{-\frac{1 + \lambda_{ph}^0 + \lambda_{sf}^0}{\lambda_{ph}^1 + \lambda_{sf}^1}\right\} \\
&= \frac{\omega}{1.2} \exp\left\{-\frac{1 + \lambda_{ph} + \lambda_{sf}}{g(\lambda_{ph} + \lambda_{sf})}\right\}, \quad (17)
\end{aligned}$$

where ω is given by Eq. (13), and we have used the relation: $\lambda_{sf}^1 = g\lambda_{sf}^0 = g\lambda_{sf}$. Note that this equation is the same as equation (3.6) of Fay and Appel,[54] except that the term λ_{ph}^1 is absent from the exponent in their expression for T_c.[55] A small value of the parameter g and a rather strong phonon contribution to the numerator in the exponent in Eq.(17) lead to small values of $T_c \lesssim 10^{-2}K$ for the $p-$wave pairing in contrast to the conclusion reached in Ref.22. The value $T_c \lesssim 10^{-2}K$ is similar to that obtained by Allen and Mitrović[21] for p-wave superconductivity in Pd. If the assumption $W^{(1)} = gW^{(0)}$ is valid, then the inclusion of antiferromagnetic spin fluctuations (replacing λ_{sf} by λ_{sf}^{af}) would lead to similar results.

V.   SUMMARY AND CONCLUSIONS

The state of hcp Fe under moderately high pressure (≤ 60 GPa) is currently riddled with controversial results that need to be resolved and understood. The initial experimental result by Shimizu et al.[1] indicating superconductivity between 15 and 30 GPa has been verified recently[2] for a pressure of 22.5 GPa, where the maximum T_c of 2 K was observed. Experimental measurements of Raman spectra are also reported.[56,57] The observation of a second Raman peak besides that due the Raman active E_{2g} mode in hcp Fe has been assigned to disorder induced phonon scattering,[56,57] although, based on density functional calculation, the possibility of antiferromagnetic order up to a pressure of approximately 60 GPa has also been suggested.[58] Normal state resistivity measurements by Jaccard et al. show a $T^{5/3}$ temperature dependence at low temperature, which is predicted by a nearly ferromagnetic Fermi-liquid model. The earlier Mössbauer study of hcp Fe under pressure had failed to reveal any local magnetic moment,[25,29] and results of theoretical calculations are dependent on the treatment of the exchange and correlation potentials used in the calculations. In view of this, we have adopted the same approach as Mazin et al.[14]: we assume nonmagnetic state under pressure and examine the electron-phonon coupling as a function of the lattice parameter.

The results of our study can be summarized as follows: (i) The Hopfield parameter η increases steadily with pressure, showing a wider variation for the linear response calculation than obtained via the RMT approximation (both in our LMTO-RMT calculation and in that of Mazin et al.[14]). (ii) Below volumes ~50 a.u. per atom (above estimated pressures ~ 160 GPa) phonons

stiffen rapidly, bringing the T_c down (somewhat faster than what is suggested in Ref.14). (iii) T_c's based on the s-wave electron-phonon coupling, and maximum possible estimates of μ^* are higher than the experimental values (iv) The range of volume where superconductivity appears is much broader in the calculations than what is observed, in agreement with the result of Ref.14. (v) Inclusion of ferromagnetic/antiferromagnetic spin fluctuations, and scattering from magnetic impurities can all bring the calculated values of T_c down to the range of observed values, but cannot substantially improve the agreement between the calculated and the experimental pressure/volume range of the superconducting phase (Fig.5). (vi) A simplified treatment of p-wave pairing due to electron-phonon and spin fluctuation interactions yields a very small T_c (≤ 0.01 K), in contrast with the claim made in Ref.22.

The role of impurities remains somewhat puzzling as well as of vital interest at present. The initial results of Shimizu *et al.*[1] showed very high normal state residual resistivity ($\sim 40\mu\Omega$cm), indicating the presence of substantial defects in the samples studied. More recent measurements[2] with purer samples (with residual resistivity 50 times smaller) show the same maximum T_c at the same pressure. If the impurities in the earlier studied samples were magnetic this would rule out electron-phonon s-wave coupling as the primary mechanism of

superconductivity. However, Jaccard *et al.*[2] also notice that superconductivity in their samples is unusually sensitive to disorder, developing only when the electronic mean free path exceeds a threshold value. They find the normal state resistivity to be characteristic of a nearly ferromagnetic metal, but our calculation of p-wave superconducting T_c in the presence of ferromagnetic spin fluctuations and electron-phonon interactions yields values less than 10^{-2} K, similar to that for Pd obtained by Allen and Mitrović.[21]

Our calculations seem to rule out both s- and p-wave superconductivity in hcp Fe. Electron-phonon mediated s-wave superconductivity should persist, in severe disagreement with experiment, beyond pressures of 200 GPa even in the presence of spin fluctuations. The possibility of d-wave superconductivity mediated by antiferromagnetic spin fluctuations remains to be explored. A d-wave superconductivity would be consistent with the observation[2] that superconductivity in hcp Fe seems to be extreemly sensitive to disorder. Low temperature specific heat measurements can further clarify this issue.

ACKNOWLEDGMENTS

* on leave from Brock University, St. Catharines, Ontario, CANADA L2S 3A1: bose@newton.physics.brocku.ca

[1] K. Shimizu, T. Kimura, S. Furomoto, K. Takeda, K. Kontani, Y. Onuki, and K. Amaya, Nature (London), **412**, 316 (2001); see also S.S. Saxena and P.B. Littlewood, Nature (London), **412**, 290 (2001).

[2] D. Jaccard it et al., cond-mat/0205557.

[3] D.G. Pettifor, J. Phys. C **3**, 367 (1970).

[4] O.K. Andersen *et al.*, Physica **86-88**B, 249 (1977).

[5] O.K. Andersen, O. Jepsen, and D. Glötzel, in *Highlights of Condensed Matter Theory*, edited by F. Bassani *et al.* (North-Holland, Amsterdam, 1985), p.59.

[6] K.A. Gschneider, in *Solid State Physics* **16**, edited by F. Seitzand D. Turnbull (Academic Press, New York 1964), 275.

[7] B. Stritzker, Phys. Rev. Lett. **42**, 1769 (1979).

[8] J. Appel, D. Fay, and P. Hertel, Phys. Rev. B **31**, 2759 (1985).

[9] S.K. Bose, J. Kudrnovský, I.I. Mazin, and O.K. Andersen, Phys. Rev. B **41**, 7988 (1990).

[10] G. Steinle-Neumann, L. Stixrude, and R.E. Cohen, Phys. Rev. B **60**, 791 (1999).

[11] R.E. Cohen, S. Gramsch, S. Mukherjee, G. Steinle-Neumann, and L. Stixrude, cond-mat/0110025.

[12] E.P. Wohlfarth, Phys. Lett. **75A**, 141 (1979).

[13] Ref.5, TABLES III-VII.

[14] I.I. Mazin, D.A. Papaconstantopoulos, M.J. Mehl, Phys. Rev. B **65**, 100511 (R) (2002).

[15] O. Jepsen *et al.*., Phys. Rev. B **12**, 3084 (1975).

[16] R. Lübers it et al., Science **287**, 1250 (2000).

[17] H.K. Mao *et al.*, J. Geophys. Res. **95**, 21 737 (1990).

[18] The normal state residual resistivity of the samples used by Shimizu *et al.*[1] were rather high ($\sim 40\mu\Omega$cm). But more recently[2], the 2 K transition at 22.5 GPa has been verified for much purer samples with residual resistivities that are about 50 times lower.

[19] S.Y. Savrasov, Phys. Rev. B **54**, 16470 (1996).

[20] S.Y. Savrasov, and D.Y. Savrasov, Phys. Rev. B **54**, 16487 (1996).

[21] P.B. Allen and B. Mitrović, *Solid State Physics*, edited by H. Ehrenreich, F. Seitz, and D. Turnbull (Academic, New York 1982), vol. 37, p.1.

[22] T. Jarlborg, cond-mat/0112382.

[23] A.P. Jephoat, H.K. Mao, and P.M. Bell, J. Geophys. Res. **91**, 4677 (1986).

[24] W.A. Bassett and E. Huang, Science **238**, 780 (1987).

[25] R.D. Taylor and M.P. Pasternak, and R. Jeanloz, J. Appl. Phys. **69**, 6126 (1991).

[26] M. Ekman, B. Sadigh, K. Einarsdotter, and P. Blaha, Phys. Rev. B **58**, 5296 (1998).

[27] J.P. Perdew, J.A. Chevary, S.H. Vosko, K.A. Jackson, M.R. Pederson, D.J. Singh, and C. Fiolhais, Phys. Rev. B **46**, 6671 (1992).

[28] J. P. Perdew, K. Burke, and M. Ernzerhofer, Phys. Rev. Lett. **77**, 3865 (1996).

[29] G. Cort, R.D. Taylor and J.O. Willis, J. Appl. Phys. **53**, 2064 (1982).

[30] P. Söderland, J.A. Moriarty, and J.M. Willis, Phys. Rev. B **53**, 14063 (1996).

[31] L. Stixrude, R.E. Cohen, and D.J. Singh, Phys. Rev. B **50**,

6442 (1994).

[32] S.Yu. Savrasov, and D.Yu. Savrasov, Phys. Rev. B **46**, 12181 (1992).

[33] P.E. Blöchl *et al.*, Phys. Rev. B **49**, 16223 (1994).

[34] F. Birch, J. Geophys. Res. **457**, 227 (1952).

[35] F.D. Murnaghan, Proc. Nat. Acad. Sci. USA **30**, 244 (1944).

[36] D. Alfé, G.D. Price, and M.J. Gillan, Phys. Rev. B **64**, 045123 (2001).

[37] G. Kresse, J. Furthmüller, and J. Hafner, Europhys. Lett. **32**, 729 (1995).

[38] P.B. Allen, Phys. Rev. B **3**, 305 (1971).

[39] V.J. Minkiewicz, G. Shirane, and R. Nathans, Phys. Rev. **162**, 528 (1967).

[40] G.D. Gaspari and B.L. Gyorffy, Phys. Rev. Lett. **28**, 801 (1972).

[41] D. Glötzel, D. Rainer, and H.R. Schober, Z. Phys. B **35**, 317 (1979).

[42] H.L. Skriver and I. Mertig, Phys. Rev. B **32**, 4431 (1985).

[43] D.J. Scalapino in: *Superconductivity*, edited by R.D. Parks (Marcell Dekker Inc., New York 1969), vol. 1, Ch. 10, p. 449.

[44] W.E. Pickett, Phys. Rev. **B 26**, 1186 (1982).

[45] A. Jephcoat *et al.*, J. Geophys. Res. **91**, 4677 (1986).

[46] H.K. Mao *et al.*, Science **292**, 914 (2001).

[47] N.F. Berk and J.R. Schrieffer, Phys. Rev. Lett. **17**, 433 (1966).

[48] S.V. Vonsovsky, Yu.A. Izyumov, and E.Z. Kurmaev, *Su-perconductivity of Transition Metals*, Springer Series in Solid-State Sciences 27 (Springer-Verlag, Berlin 1982), section 3.9.2, p. 171.

[49] P.W. Anderson, J. Phys. Chem. Solids **B 11**, 26 (1959).

[50] A.A. Golubov and I.I. Mazin, Phys. Rev. **B 55**, 15146 (1997).

[51] O.V. Dolgov and A.A. Golubov, Int. J. Mod. Phys. **B 1**, 1089 (1989).

[52] C. Jiang, J.P. Carbotte, R.C. Dynes, Phys. Rev. **B 47**, 5325 (1993).

[53] P.B. Allen, Phys. Rev. B **B 13**, 1416 (1976).

[54] D. Fay and J. Appel, Phys. Rev. B **B 22**, 3173 (1980).

[55] Jarlborg[22] claims to use this same equation, but uses the same coupling parameter λ_{sf}^0 both in the numerator and denominator of the argument of the exponential function, and consequently obtains a T_c much higher than the correct equation would yield.

[56] S. Merkel, A.F. Goncharov, H. Mao, P. Gillet, and R.J. Hemley, Science **288**, 1626 (2000).

[57] A.F. Goncharov *et al.*, cond-mat/0112404.

[58] G. Steinle-Neumann, L. Stixrude, R.E. Cohen, and B. Kiefer, cond-mat/0111487.

[59] The values quoted for $N(0)_{Fe}$[14] and $N(0)_{Ru}$[15] are obtained via different methods: LAPW[14] and LMTO.[15] Using the same method to calculate both DOSs would result in a ratio that is 10% smaller, giving $\lambda_{ph} = 0.5$ for Fe, and a $T_c \sim 5$ K.